

## Dose gradient assessment at the new CERN CHARM irradiation facility

A. Infantino\*, C. Cangialosi, M. Krawina, M. Brucoli, M. Brugger, J.P. De Carvalho Saraiva, S. Danzeca

European Organization for Nuclear Research (CERN), Geneva 23, CH1211 Geneva, Switzerland

### ARTICLE INFO

#### Keywords:

CERN  
CHARM  
Mixed field  
FLUKA  
RPL  
RadFET

### ABSTRACT

CERN CHARM facility provides a unique complex radiation environment characterized by particle energy spectra representative of high-energy accelerators, ground and atmospheric conditions and space applications. CHARM is conceived to be an irradiation facility for the qualification of large electronic systems and components in a mixed field radiation environment generated from the interaction of a 24 GeV/c proton beam with a copper or aluminium target. A movable shielding made of layers of concrete and iron allows changing the hardness and the particle population (neutron, proton, kaon, pion, muon, electron, positron, and photon) in predefined test locations. To ensure a full representativeness and reproducibility of the tests, an accurate dosimetry of the complex mixed irradiation field is mandatory. The significant size of the available test area, the multiple facility configurations as well as the strong radiation gradient present in some of the test locations make the radiation monitoring a challenge. This work provides a first characterization of the absorbed dose gradient in two specific test locations: T0, a high dose rate test location close the target revolver; R11, a standard test location for irradiation tests on electronics equipment and devices. Experimental measurements conducted with RPL dosimeters and pMOS RadFET sensors were coupled with FLUKA Monte Carlo simulation. The concluding comparison shows an overall good agreement, considering the strong dose gradient and the limitation of the dosimeters in the mixed field environment.

### 1. Introduction

The irradiation facility called CHARM (CERN High energy AccelRator Mixed field/facility) has been built at CERN between 2013 and 2014, in the framework of the Radiation to Electronics (R2E) project, with the main purpose of testing electronic equipment in a radiation field similar to the one occurring at CERN accelerators (e.g. in the Large Hadron Collider - LHC). This facility is not only used for testing devices within accelerator representative environments, but its available radiation fields are also characteristics for ground and atmospheric environments as well as for space environments (Mekki et al., 2016). With regard to the accelerator environment, the complex radiation field of stray particles present within CERN accelerators is composed by a mix of charged and neutral hadrons, photons, muons and electrons/positrons of energies ranging from GeVs down to thermal energies: electronic devices and systems operating in such an environment are simultaneously affected by Single Event Effects (SEEs), Total Ionizing Dose (TID)<sup>1</sup> and Displacement Damage (DD). The same particle environment can be found in the CHARM mixed field.

A 24 GeV/c pulsed proton beam, extracted from the CERN Proton Synchrotron (PS), is directed along T8 beam-line in the PS East Area Hall. The beamline passes first through the IRRAD proton facility (CERN, 2017a; Gkotse et al., 2014) and finally delivers the proton beam to CHARM (CERN, 2017b). The mixed field is generated within the irradiation room (Fig. 1) by the interaction of the proton beam with a cylindrical target (50 cm length, 8 cm diameter) of different materials (copper or aluminium). The device under test (DUT) can be placed in more than 14-standard test locations (labelled from T0 to 14) and the particle spectra can be further modulated in the different positions through a movable shielding made of  $2 \times 20$  cm slabs of concrete and  $2 \times 20$  cm slabs of iron. The size of the available test area is such that also large objects can be irradiated such as a complete accelerator control or powering system (e.g. LHC power converters) but also full-scale satellites, and parts of cars or planes. The proton beam is extracted from the PS in a variable number of spills, typically from 1 up to 5, during the so-called PS “super-cycle”, lasting  $\sim 45$  s. The number of primary protons interacting with the target (Protons On Target - POT) is measured by a secondary emission counter (SEC) placed upstream the

\* Corresponding author.

E-mail address: [angelo.infantino@cern.ch](mailto:angelo.infantino@cern.ch) (A. Infantino).

<sup>1</sup> i.e. the total absorbed dose [Gy].

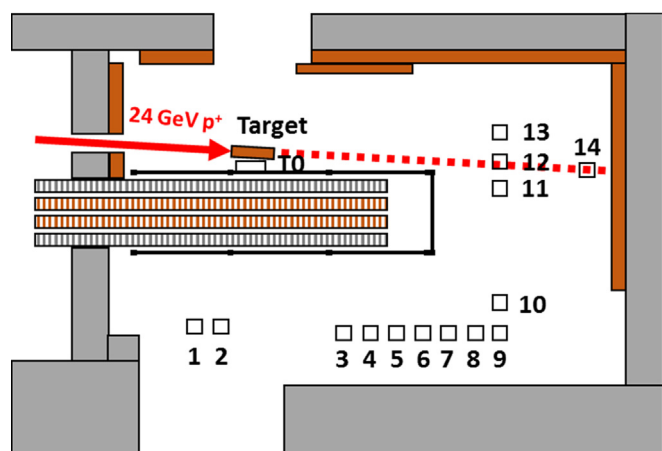


**Fig. 1.** Sketch of the CHARM facility irradiation room. The 24 GeV/c proton beam interacts with a copper (or aluminium) target and generates the mixed field within the test area. Standard test locations are labelled from T0 to 14, represented in the picture by rectangles. The four slabs of the movable shielding are indicated with the grey (concrete) and red (iron) dashed texture.

IRRAD facility. Further details about the CHARM facility can be found in Mekki et al. (2016), Thornton (2016).

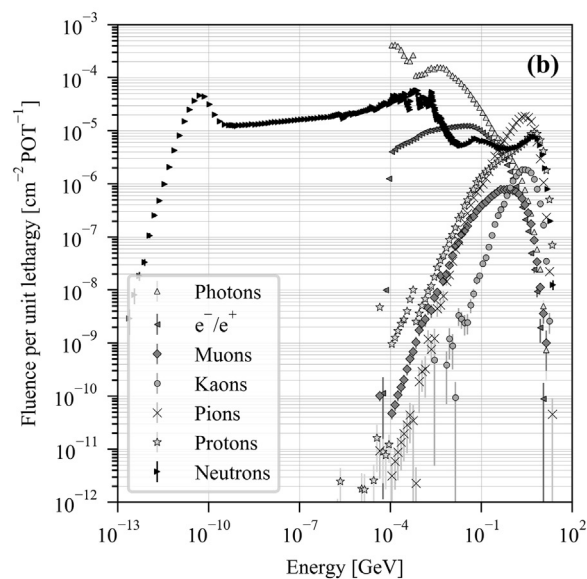
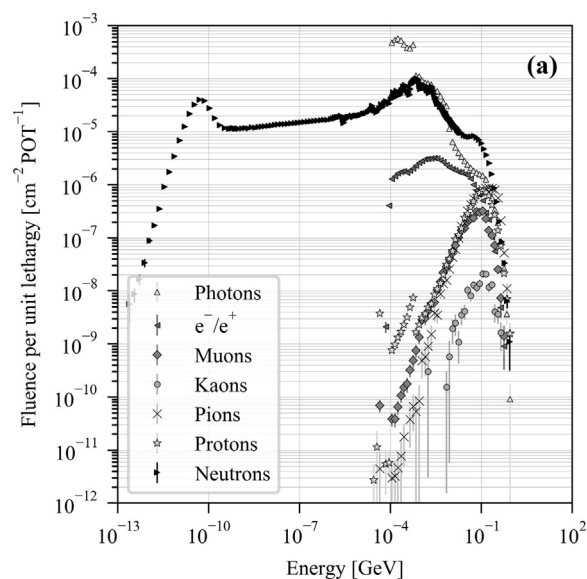
In opposition to conventional test facilities where irradiation tests are performed either using mono-energetic particle beams or sources, with only one or few discrete energies, or using particle field (e.g. neutron testing with a broad energy spectrum), the unique key feature of CHARM is that the radiation field is of mixed nature (multitude of particles and energies) and expands all over the radiation area.

Fig. 2 reports the typical radiation environment in the test locations 1 (Fig. 2a) and 11 (Fig. 2b) while Mekki et al. (2016) reports the comparison between the particle environment in the LHC tunnel and shielded alcoves for electronics with some reference positions/configurations of the CHARM facility.

This complex radiation field poses important challenges in the calibration and dosimetry of the facility, which is a key point for ensuring the reliability and reproducibility of the tests. Furthermore, some of the test locations are affected from a very strong absorbed dose gradient (in the following just “dose”) for which an accurate characterization is mandatory to meet the already mentioned required quality standards. In addition, the detailed knowledge of the dose field in test locations affected by this gradient is crucial for the goodness of the test results, particularly with regard to all those applications in which the exact knowledge of the delivered dose is fundamental (e.g. electronic component lifetime, material science, etc).

In literature, several works about the dose assessment in mixed  $n$ - $\gamma$  or  $\beta$ - $\gamma$  field can be found (Angelone et al., 2011): these papers usually refer to fields composed of two particle species, with lower energies and lower dose rates compared to the CHARM particle and energy spectrum. At the best of our knowledge, just a few works report about dose measurements in a high-energy mixed field (Mekki et al., 2016; Vincke et al., 2007; Bruccoli et al., 2017). Vincke et al. (2007) report about the use of Alanine and RPL (Radio-photo-luminescence) dosimeters at CERF facility (CERN-EC High Energy Reference field Facility), where the mixed field is generated from the interaction of a 120 GeV/c proton beam on a copper target. Mekki et al. (2016), reports about the first calibration campaign conducted at CHARM which can be considered the baseline for the present work. Finally, Bruccoli et al. (2017), reports about measurements of the TID with Floating Gate dosimeters in the CHARM mixed field and the further comparison with RadFET (Radiation-sensing field-effect transistor) sensors.

This work aims to characterize the CHARM dose field in critical test locations affected by a strong dose gradient by means of FLUKA Monte Carlo (MC) simulation (Ferrari et al., 2005; Böhlen et al., 2014) and



**Fig. 2.** Particle environment at CHARM: test location 1 (a) and 11 (b), copper target without shielding. Fluence is normalized by the number of primary protons interacting with the copper target (POT). The shape of the particle spectra in T0 results to be very similar to the one of positions 11–13 while, in absolute terms, higher fluences can be found due to the vicinity to the target.

experimental measurements conducted using RadFET sensors and RPL dosimeters. The challenges and the main achievements of the present work will be discussed in the following sections.

## 2. Materials and methods

### 2.1. Dosimeters

In this work, two different kinds of dosimeters were used: RPL and RadFET. The main features of the different dosimeters are discussed in the following.

RPL dosimeters consist of silver-activated phosphate glass (Vincke et al., 2007). The radiation measurement procedure relies on the creation of luminescence centres in the presence of ionizing radiation. The amount of these centres can be correlated to the dose received by the dosimeters (Yamamoto, 2011). The read-out of the amount of luminescence centres is based on a UV light excitation of the dosimeter.

The dose range covered by RPL dosimeters currently used at CERN is between 1 Gy and 100 kGy (CERN HSE-RP group, private communication).

The calibration of RPL dosimeters is conducted internally at CERN, by the HSE-RP group, using a  $^{60}\text{Co}$  gamma-field. During the calibration irradiation, the dosimeters are placed in a polyethylene (PE) container of 3 mm thickness. The photons impinging on the 3 mm PE wall produce a photon-electron equilibrium, similar to the one created in air. Hence, the dose value obtained by the dosimeter readout procedure is given as dose-in-air which is deposited by the calibration source: i.e. the measured dose (induced by an arbitrary irradiation field) is interpreted as the photon dose-in-air which is required to produce the observed readout signal (CERN HSE-RP group, private communication). The same containers were used for the measurement campaign reported in this work. For a gamma field, the mass absorption coefficient in air and in Si are approximately the same in a very broad energy range (100 keV up to a few MeV). At the energy used for the calibration,  $^{60}\text{Co}$  gamma lines, the dose in air and in Si are approximately the same (Ravotti, 2018). However, the desired result of the dosimeter readout procedure is not the dose-in-air caused by a photon source but the dose deposited in air by the given (arbitrary) particle field. Since the dosimeters are calibrated to a photon field a correction of the dosimeter readout value might be required to obtain the real dose, which is deposited in air by the given particle field. Nevertheless, the RPL response to other particles than photons and electrons is not well understood, especially in the high-energy range. Indeed, as reported by Vincke et al. (2007), up to now it is not clear how reliably these dosimeters can operate in mixed high-energy radiation fields. The canonical calibration methodology would require a dedicated calibration for each radiation in term of relative response to  $^{60}\text{Co}$ , however this approach is unrealistic for a LHC-like environment such as the CHARM one. Indeed, the availability of primary calibrated sources is mainly restricted to gamma radiation. Monoenergetic beams of protons can be found in some test facilities around the world (e.g. PSI, TRIUMF, etc.) but energies are usually limited to a few hundreds of MeV. Above these energies, the availability of proton beams is limited to a few high-energy physics laboratories, for which the possibility to have a pure proton field is limited or impracticable. Monoenergetic neutron beams are mainly limited from thermals to a few tens of MeV, with discrete energies: therefore, it is not possible to cover experimentally the full energy range of an LHC-like environment. With regard to other particles (pion, muon, etc) the availability of mono-energetic beams is limited to test facilities, which do not represent anyway a primary calibration sources. An evaluation of the relative response to  $^{60}\text{Co}$  is therefore only possible through MC simulation. Vincke et al. (2007) performed a detailed characterization through MC of a type of RPL formerly used at CERN. In addition, experimental measurements at the CERF facility were performed in an irradiation setup such that the electromagnetic component was the predominant component of the radiation field: therefore, the RPL response in the mixed field was assumed to be the same of the one obtained during calibration. The irradiation setup of the measurements reported in this publication is such that the electromagnetic component cannot be considered the main contribution to the absorbed dose being ~50% of the total. Finally, a characterization of the response of the currently used RPL glass, using FLUKA simulation, is ongoing and will be reported in a further publication.

RadFETs are P-channel MOSFETs optimized to monitor the TID and are used at CERN in zero bias mode (Holmes-Siedle et al., 1985; Mekki et al., 2009). Details on the RadFET geometry can be found in Jaksic et al. (2006). Ionizing particles passing through the gate oxide transistor generate positive and negative charges. While negative charges are fast swept out from the oxide to the gate due to their high mobility, positive charges are trapped within the oxide. This build-up of positive charge within the gate Silicon dioxide is responsible for the threshold voltage shift of the dosimeters, measured at a constant drain to source current. Therefore, the observed variation is a function of the absorbed

dose (Mekki et al., 2013). RadFET are used at CERN both in active and passive mode. Active RadFET are installed in a more complex device called RadMon (Radiation Monitoring system) which includes, together with the pMOS sensors, SRAM memories for measuring the High Energy Hadrons (HEH) fluence (hadrons > 20 MeV) through Single Event Effects (SEE). In addition, it includes P-I-N diodes, for measuring the 1 MeV neutron equivalent fluence through Displacement Damage (DD) (Spiezia et al., 2014; Kramer et al., 2011; Cangialosi et al., 2018). RadMon are then connected to the CHARM control room through a patch panel, which allows the online readout of the different systems. Moreover, RadFET can be used in passive mode, without being physically installed in the bulkier RadMon system, by reading the threshold voltage shift pre- and post-irradiation. Due to their sensibility to the ambient temperature (Spiezia et al., 2014), RadFET sensors were stabilized prior each irradiation test during this campaign.

The RadFET response function has been evaluated in a  $^{60}\text{Co}$ -gamma field as reported by Mekki et al. (2013). Moreover, Mekki et al. concludes that “the  $^{60}\text{Co}$  calibration might be sufficient in a mixed particle field if uncertainties of  $\pm 25\%$  are accepted and if thin RadFET (e.g. 100 nm) are used”. The response to protons, in the energy range 30–230 MeV, was assessed at PSI (Switzerland) for different RadFET architectures, namely 400 nm and 100 nm (Spiezia et al., 2014). The latter is currently adopted in the sensors used in this work for the motivations explained in the mentioned references. Studies on the RadFET sensibility to thermal neutrons have been recently reported in Marzo et al. (In press), by comparing experimental measurements and FLUKA simulations.

Table 1 reports the main features of the two type of dosimeters used in the present work.

## 2.2. Experimental setup

In this work, experimental measurements have been conducted in two test locations, namely T0, and 11 (Fig. 1). T0 is a  $15.5 \times 13.6 \times 30.5 \text{ cm}^3$  aluminium table, installed ~10 cm from the target revolver, 90 degrees from the beam direction. This test location was recently installed at CHARM and is used for irradiation of materials and components which need to collect high-doses: on average up to ~4 kGy/day can be delivered here. Given the short distance from the target revolver, a high dose field is expected in this position: an experimental characterization of the dose field, as well as a detailed study using FLUKA simulation, is therefore mandatory for the reliability of the irradiation tests. Test location 11 (R11 in the following) is used for testing electronic equipment and components by means of an experimental rack ( $60 \times 161 \times 90 \text{ cm}^3$ ) where the boards, the power supply, and the signal cables are installed. The difference in testing among the standard test positions is given from the different particle environment available at each location, particularly when the full shielding is completely extracted: for example, R1 presents a particle environment similar to the LHC heavily shielded alcoves where the electronics are usually located (Mekki et al., 2016). On the other hand, position R11 is representative of the LHC tunnel environment as well as, in terms of

**Table 1**  
Main features of the dosimeters used in the experimental campaign.

	RPL	RadFET
<b>Detectors</b>	Silver activated metaphosphate glass	p-channel MOSFET
<b>Effect Analysis</b>	radio-photoluminescence centres UV-light exposure	TID threshold voltage shift
<b>Dimensions</b>	8 mm height, 1 mm diameter	100 nm (sensitive volume)
<b>Measured quantity</b>	Absorbed dose	Absorbed dose
<b>Calibration</b>	$^{60}\text{Co}$	$^{60}\text{Co}$
<b>Dose range</b>	1 Gy – 100 kGy	20 mGy to 20 kGy
<b>Accuracy (<math>^{60}\text{Co}</math>)</b>	~6% (k = 2)	40% (k = 2)

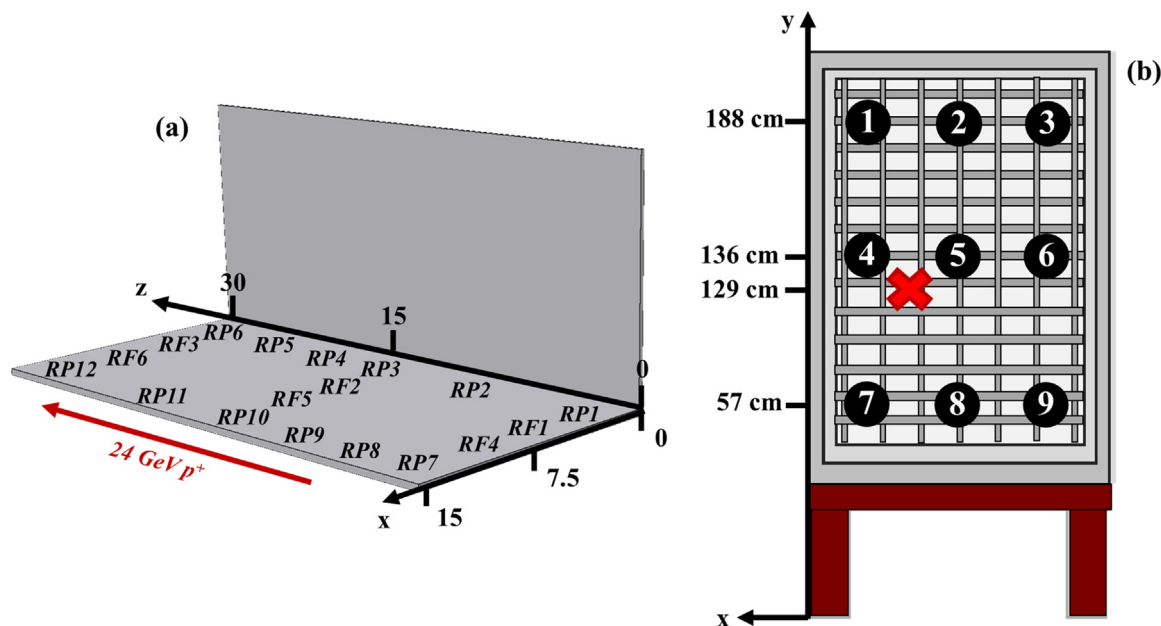


Fig. 3. Experimental setup adopted for the T0 and R11 test locations. With regard to the R11 irradiation test, the red cross indicates the beam height.

SEE rate in a deep-submicron bulk technology, of the atmospheric particle environment at flight altitude, as reported by Infantino et al. (2017a).

Fig. 3 shows the experimental setup adopted in the test locations T0 and R11. In test location T0 (Fig. 3a) 12 RPL (RP1–RP12) were placed in two different rows, along the beam direction. Due to the very small dimensions of the RPL, the dosimeters were individually placed in PE containers of 2.5 cm in diameter, 0.8 cm height: each “RP” label represent the position of these plastic containers. To further cover the T0 surface, 6 RadFET (RF1–RF6) sensors were placed in between the two rows of RPL. With regard to R11 (Fig. 3b), a 3 × 3 matrix setup was used: a metal grid was installed in the front surface of the rack, allowing, in each point, for the installation of one RadMon (or alternatively a passive RadFET) and one RPL.

In order to maximize the field intensity, the irradiation tests were conducted running the facility with the copper target with no shielding inserted. The irradiation time (no larger than 6 h) was set in order to collect a statistically meaningful amount of dose with the difference dosimeters, i.e. to collect at least the minimum readable dose (Table 1). On average, 3 spills per PS super-cycle have been extracted for a beam intensity of  $\sim 2.2E+10$  POT/s.

### 2.3. FLUKA model of the CHARM facility

FLUKA is a general purpose Monte Carlo code for modelling particle transport and interaction with matter; it covers an extended range of applications spanning from proton and electron accelerator shielding to calorimetry, dosimetry, detector design, radiotherapy and more (Ferrari et al., 2005). FLUKA simulation is routinely used at CERN in secondary beam design, energy deposition (quenching, damage), radiation damage (electronics, insulation), dosimetry, shielding activation, residual dose rates, and waste disposal (Böhlen et al., 2014). A full Monte Carlo model of the CHARM facility (Fig. 4) has been developed over the last years for integrating the experimental calibration and dosimetry, providing information about the radiation field in standard and non-standard test locations, planning experimental tests of components and equipment. More details on prior campaigns and the model can be found in Mekki et al. (2016), Thornton (2016), and Infantino (2017b).

The main key features of the model are: i) a detailed modelling of all the main parts and components of the irradiation room including the

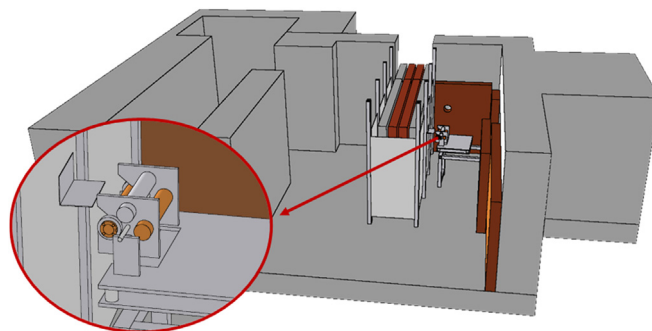


Fig. 4. FLUKA Monte Carlo model of the CHARM facility. The layout of the facility has been accurately reproduced from the original technical drawings and considers all the main components such as the movable shielding and the target revolver.

target revolver, the movable shielding, the entrance maze, the surrounding shielding; ii) an accurate description of the 24 GeV/c proton beam in terms of momentum, momentum spread, divergence, beam spot dimensions, beam direction cosines; iii) a fine tuning of the main production and transport threshold (100 keV for  $e^+/e^-$  and  $\gamma$ ; 100 keV for proton, pion, muon, kaon); iv) the use of a suitable fine Cartesian meshes (USRBIN) for the estimation of the energy deposition in the test locations of interest. The USRBIN mesh were set to cover the full area of T0 and R11, with a resolution of 1 cm in all directions: this approach allowed for a good balance between a fine resolution (for the purpose of this first assessment) and a suitable computational time for achieving an acceptable statistical uncertainty. In this first approach, the dose has been scored in air: due to the extremely small dimensions of the detectors, with respect to the full model of the facility, the scoring of the dose in these sensitive volumes would have required an extreme computational effort. A possible alternative approach would have been to setup a two-step simulation, i.e. scoring the particle spectra in the areas where the dosimeters are placed and then further transport these spectra in a dedicated Monte Carlo model of the dosimeters. Once more, as this work is intended as a first assessment of the dose gradient and a preliminary comparison with the dosimeters commonly used in the calibration of the facility, we decided to leave this second, and more complex approach, to a further stage. High-statistics simulations were

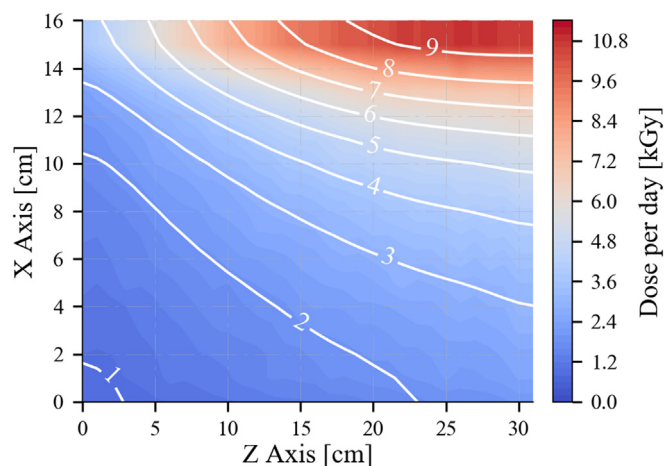


Fig. 5. Dose contour plot in T0 (FLUKA simulation). The total dose per day has been calculated considering an average irradiation of 24 h with 3 spills per PS super-cycle ( $1.92E+15$  POT/day). The beam, non-visible in this picture ( $x > 16$ ), is going toward  $z > 0$ .

performed to achieve a statically meaningful result: the maximum statistical uncertainty on the evaluated dose was  $< 5\%$  and  $< 10\%$  in T0 and R11 respectively, with the average uncertainty well below these values.

### 3. Results

#### 3.1. Position T0

Fig. 5 shows the dose contour plot for the position T0, at surface level. The picture shows, qualitatively, how a strong dose gradient is present in both x- and z-direction: from the coordinate (0,0) to (30,15) it is possible to observe a dose difference of a factor  $\sim 10$ .

To be quantitative, a detailed analysis of the dose distribution along the z-direction (beam direction) is reported in Fig. 6: considering  $x = 0$ ,  $x = 7.5$ , and  $x = 15$  cm, we can observe a variation of the dose in the z-direction from a factor  $\sim 2$  to  $\sim 3$  respectively. On the other hand, fixing the z-coordinate, the dose variation along the x-direction (perpendicular to the beam direction) at  $z = 0$  and  $z = 30$  cm is of the order of magnitude of a factor  $\sim 4$ . FLUKA simulation allows computing the dose gradient in the different directions. To compare different irradiation profiles, and to take into account the pulsed proton beam from the PS, it is suitable to report the dose gradient in units of Gy/cm/spill: the calculated dose gradient along the z-direction is, therefore,  $4.0E-02$  and

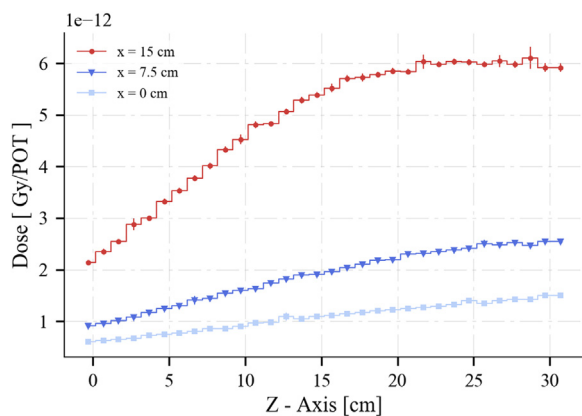


Fig. 6. Dose distribution along the z-direction (beam direction) evaluated with FLUKA simulation at  $x = 0, 7.5$  and  $15$  cm. Dose is normalized by the number of primary protons interacting with the copper target (POT).

Table 2

Comparison of the FLUKA simulation with the experimental results. The absorbed dose is normalized according to the experimental setup of Fig. 3. A total of  $2.40E+14$  POT were collected during the experimental measurement.

Detector	Experimental	FLUKA	FLUKA/Exp.
RP1	1	1	1
RP2	$1.47 \pm 0.06$	$1.1 \pm 0.3$	$0.78 \pm 0.23$
RP3	$2.00 \pm 0.08$	$1.7 \pm 0.5$	$0.85 \pm 0.24$
RP4	$2.22 \pm 0.09$	$1.9 \pm 0.5$	$0.85 \pm 0.25$
RP5	$2.61 \pm 0.11$	$2.3 \pm 0.7$	$0.87 \pm 0.26$
RP6	$2.66 \pm 0.11$	$2.3 \pm 0.6$	$0.86 \pm 0.25$
RP7	1	1	1
RP8	$1.14 \pm 0.05$	$1.4 \pm 0.4$	$1.2 \pm 0.3$
RP9	$1.92 \pm 0.08$	$2.0 \pm 0.6$	$1.1 \pm 0.3$
RP10	$2.21 \pm 0.09$	$2.3 \pm 0.7$	$1.1 \pm 0.3$
RP11	$2.45 \pm 0.10$	$2.7 \pm 0.8$	$1.1 \pm 0.3$
RP12	$2.15 \pm 0.09$	$2.7 \pm 0.8$	$1.3 \pm 0.4$
RF1	1	1	1
RF2	$1.7 \pm 0.5$	$1.7 \pm 0.5$	$1.0 \pm 0.4$
RF3	$2.0 \pm 0.6$	$1.9 \pm 0.5$	$1.0 \pm 0.4$
RF4	1	1	1
RF5	$1.6 \pm 0.5$	$1.4 \pm 0.4$	$0.9 \pm 0.3$
RF6	$2.1 \pm 0.6$	$2.0 \pm 0.6$	$0.9 \pm 0.4$

$5.0E-03$  Gy/cm/spill at  $x = 0$  and  $x = 15$  cm respectively.

It is important to underline that, even if not reported in this work, the dose gradient is not restricted to the x/z-direction: indeed, a similar gradient is present in the y-direction as well.

Table 2 reports the comparison of FLUKA simulation with the experimental measurements. Due to the lack of knowledge about the response function of the RPL dosimeters to all the particle composing the CHARM radiation environment, results were compared in a relative term. The same approach was used for the RadFET sensors. Results in Table 2 were normalized according to the setup shown in Fig. 3: the reading of the first dosimeter in a row was used as normalization factor so that the gradient in the z-direction can be calculated. Finally, the ratio between FLUKA simulation and the experimental measurements has been calculated. The uncertainty of the ratio FLUKA/experimental was calculated by a quadratic propagation of the Monte Carlo statistical uncertainty, the calibration uncertainty of the dosimeters (referring to the calibration in  $^{60}\text{Co}$ ) and the uncertainty of the SEC, 20% at 1-standard deviation. The comparison of the absolute absorbed dose is reported in Fig. 7. All the dosimeters agree within a factor 1.3 with FLUKA simulation: we find this agreement satisfactory since, due to the relative position of the dosimeters with respect to the target and the strong dose gradient in both x/z-direction, small uncertainty in the positioning of the dosimeters can lead to a significant difference in the dose estimation. By taking into account the irradiation conditions during the measurement, it is possible to assess the dose gradient in absolute terms: from Fig. 7a, a dose gradient of  $\sim 6$  Gy/cm was found; from Fig. 7b, the experimental values and FLUKA simulation give a dose gradient of  $\sim 18$  and  $30$  Gy/cm respectively. One more time, the latter values show how small uncertainties in the positioning of the dosimeters can lead to significant difference in the dose.

Despite the differences in absolute terms, the trend followed by the experimental and the simulation data is very similar: indeed, data in Table 2 show how, in a relative term, the data sets agree within uncertainties. This systematic difference between absolute absorbed doses might be explained from the lack of a canonical calibration for the mixed field, i.e. the unknown response function to all the particle of the radiation environment.

#### 3.2. Position R11

Fig. 8 shows the dose contour plot for the front surface of R11. From this figure we can observe that the beam crosses the surface of the rack and consequently its full depth: the isodose lines show how within a

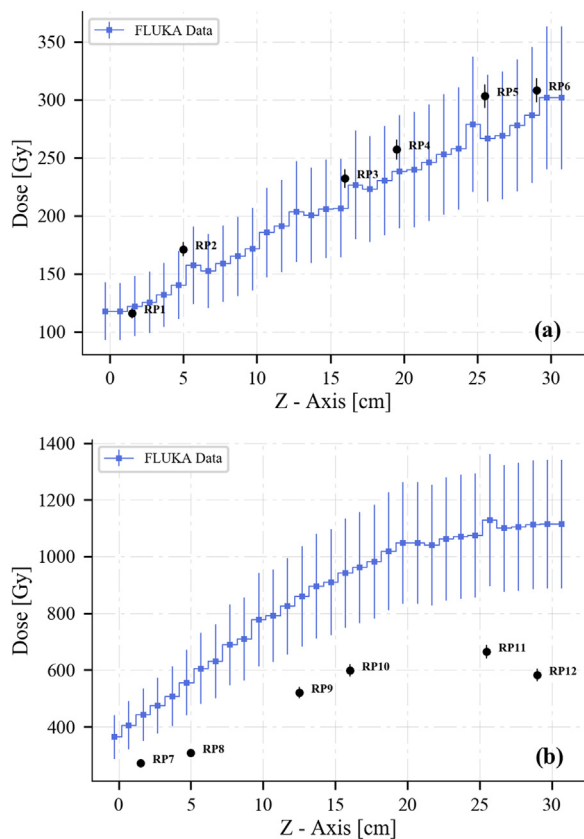


Fig. 7. FLUKA- and experimental-evaluated dose distribution along the z-direction (beam direction) where the x-coordinates correspond to the two rows of RPL dosimeters on the table. RadFET sensors are not reported in the plots since they are not positioned at the same x-coordinates as the RPL ones.

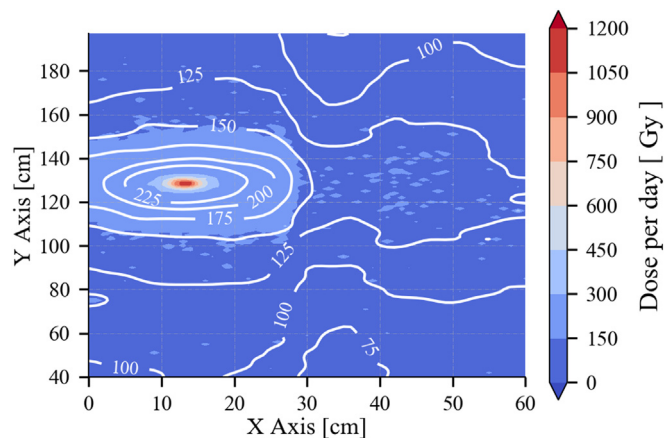


Fig. 8. Dose contour plot for the R11 front surface (FLUKA simulation). The total dose per day has been calculated considering an irradiation of 24 h with 3 spills per super-cycle ( $1.92E+15$  POT/day).

20 × 10 cm area the dose can vary from ~225 Gy to almost 1200 Gy. Fig. 9 allows a detailed overview of the FLUKA dose profile along the x-direction, at beam (129 cm) and detector (136 cm) height: considering the centre of the beam spot, the difference in height between the beam spot and the dosimeters (just 7 cm) produces a difference in dose of a factor ~6. Furthermore, at beam height, the dose varies of a factor ~6, in the x-direction, within a range of ± 10 cm from the beam spot (Fig. 9).

As already shown for position T0, Table 3 reports the results in a relative term by normalizing the data accordingly to the experimental

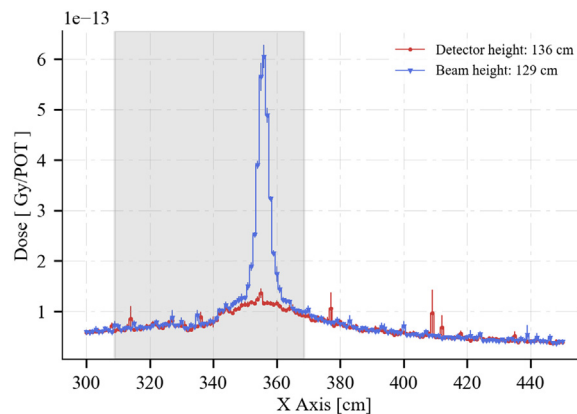


Fig. 9. Dose distribution assessed with FLUKA simulation at beam and detector height. The dose is normalized by the number of primary protons interacting with the copper target (POT). The grey rectangle represents the rack width in the absolute CHARM reference system: the proton beam cross completely the rack. The x-axis reports the absolute x-coordinate as in the FLUKA reference system, thus it results mirrored with respect to Fig. 8.

setup of Fig. 3b. Once again, despite the differences in absolute value, the profile followed by the different datasets is the same within statistical uncertainties.

Position R11 allows directly comparing RPL and RadFET measurements given that the dosimeters were placed in the same position: a systematic difference of 46% was observed, on average in the mixed field, between RPL and RadFET measurements. A similar result was found in position T0 in a preliminary measurement campaign conducted in 2016 (not reported) where RPL and RadFET were stacked in 6 different locations: by the time, the average ratio RPL/RadFET was 30%. Finally, a systematic difference < 15% was found in experimental measurements conducted at CERN in a pure  $^{60}\text{Co}$  field: considering the achievable accuracy (Table 1) in these specific irradiation conditions the difference is within the experimental uncertainty, whereas this is not the case anymore for the mixed field.

As for position T0, by plotting the FLUKA dose profile vs the experimental results it is possible to observe how the latter follow the predicted distribution: as example, Fig. 10 shows the dose profile for the central row (position 4, 5, 6). Close to the beam halo, small uncertainty in the positioning can lead to large uncertainty in the dose measurement.

#### 4. Conclusions

CERN High energy Accelerator Mixed field/facility, CHARM, is conceived to be an irradiation facility for the qualification of large electronic systems and components in a mixed field radiation environment representative of the accelerator field as well as ground, avionics and space applications. The mixed field of neutron, proton, kaon, pion, muon, electron, positron and photon is generated from the interaction of a 24 GeV/c proton beam with a copper or aluminium target. A movable shielding made of layers of concrete and iron allows changing the hardness and the particle population in predefined test locations. These unique conditions pose important challenges in the accurate calibration and dosimetry of the facility, which is a key point for ensuring the reliability and reproducibility of tests. Furthermore, the detailed knowledge of the dose field in test locations affected by a significant dose gradient is crucial for the goodness of the test results, particularly with regard to all those applications in which the exact knowledge of the delivered dose is fundamental (e.g. electronic component lifetime, material science, etc). To support the calibration of the facility, a FLUKA Monte Carlo model of the full CHARM facility has been developed in the last years for integrating the experimental dosimetry, providing information about the radiation field in standard and

**Table 3**

Relative dose measured at R11 and comparison with FLUKA simulation. A total of  $2.40E+14$  POT were collected during the experimental measurements. RadFET measurement at position 3 was affected by a readout error which did not allow to properly evaluate the dose in that position.

Position	RPL	RadFET	FLUKA	FLUKA/RPL	FLUKA/RadFET
1	1	1	1	1	1
2	$0.95 \pm 0.04$	$0.82 \pm 0.23$	$0.86 \pm 0.25$	$0.90 \pm 0.26$	$1.0 \pm 0.4$
3	$0.73 \pm 0.03$	n/a	$0.94 \pm 0.27$	$1.3 \pm 0.4$	n/a
4	1	1	1	1	1
5	$0.81 \pm 0.03$	$0.66 \pm 0.19$	$0.63 \pm 0.18$	$0.78 \pm 0.22$	$0.9 \pm 0.4$
6	$0.66 \pm 0.03$	$0.61 \pm 0.17$	$0.60 \pm 0.17$	$0.91 \pm 0.26$	$1.0 \pm 0.4$
7	1	1	1	1	1
8	$0.74 \pm 0.03$	$0.78 \pm 0.22$	$0.61 \pm 0.18$	$0.82 \pm 0.25$	$0.8 \pm 0.3$
9	$0.83 \pm 0.04$	$0.86 \pm 0.24$	$0.82 \pm 0.26$	$1.0 \pm 0.3$	$1.0 \pm 0.4$

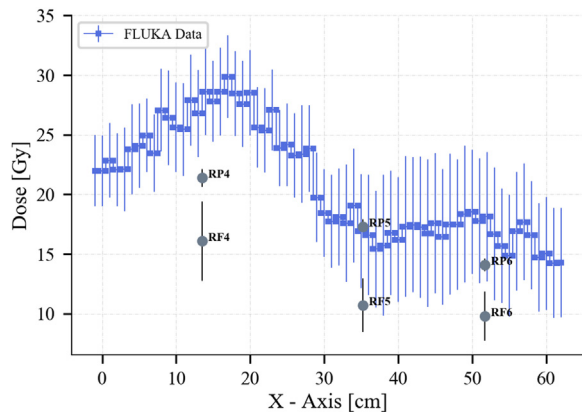


**Fig. 10.** FLUKA- and experimental-evaluated dose distribution along the x-direction (rack width) at  $y = 136$  cm (position 4, 5, 6).

non-standard test locations, planning experimental tests of components and equipment.

In this work, the first experimental evaluation of the dose gradient in a few test locations of the CHARM facility and the comparison of the results with FLUKA simulation were reported. Two different test locations were studied: T0, a high dose rate test location close the target revolver; R11, a standard test location for irradiation tests on electronics equipment and devices. Experimental measurements were conducted with RPL dosimeters and RadFET sensors. Both dosimeters are calibrated in a pure  $^{60}\text{Co}$  field, while the response in the mixed field is not well known. With regard to the T0 test location, FLUKA simulation allowed for a detailed study of the dose field: the simulation shows how close to the target revolver, the dose field can vary up to a factor  $\sim 3$  in the beam direction and, overall, up to a factor  $\sim 10$  considering the full surface of the table. With regard to the experimental measurements, both families of dosimeters give a good agreement when compared in relative terms: considering the strong dose gradient (up to 30 Gy/cm during the irradiation test) and the limitation of these kind of dosimeters in the mixed field the agreement with FLUKA is satisfactory.

In test location R11, FLUKA simulation allowed again for a detailed assessment of the dose field on the surface of the rack: indeed, due to the physical dimensions of the dosimeters, reaching the same spatial resolution and level of detail would be impracticable from an experimental point of view. Monte Carlo simulation shows how in an area of  $20 \times 10$  cm from the beam spot the dose can vary up to a factor  $\sim 6$ . Overall, FLUKA simulation and experimental measurements agree within a factor 2, with again RPL better matching the predicted dose.

In conclusion, the present work reports about the preliminary characterization of the dose gradient within the CHAM facility. Results show how a detailed knowledge of the dose field in test locations affected by a strong dose gradient is crucial for ensuring the reliability and reproducibility of tests. Indeed, in these test locations, small uncertainty in the positioning of the device under test can lead to a

significant difference in the cumulated dose, possibly compromising the goodness of the test itself. A validated FLUKA Monte Carlo model allows knowing the radiation field with a level of detail which is impracticable with experimental measurements and therefore to properly support the dosimetry of the facility. Moreover, FLUKA simulation can be used for retrieving the response of the dosimeter in a complex mixed field for which a canonical calibration, in this high-energy domain, results unrealistic.

### Acknowledgements

The Authors would like to acknowledge Dr. Diego Di Francesca, Dr. Federico Ravotti, Dr. Ruben Garcia Alia, Dr. Francesco Cerutti from CERN for their contribution and for the very useful discussions and suggestions. In addition, the Authors thank the HSE-RP section of CERN, particularly Dr. Helmut Vincke, Dr. Julia Brigitta Trummer and Dr. Isabel Brunner, for their cooperation and inputs.

### References

- Angelone, M., Batistoni, P., Bedogni, R., Chiti, M., Gentile, A., Esposito, A., Pillon, M., Villari, R., 2011. Mixed n-g fields dosimetry at low doses by means of different solid state dosimeters. *Rad. Meas.* 46, 1737–1740.
- Böhlen, T.T., Cerutti, F., Chin, M.P.W., Fassò, A., Ferrari, A., Ortega, P.G., Mairani, A., Sala, P.R., Smirnov, G., Vlachoudis, V., 2014. The FLUKA code: developments and challenges for high energy and medical applications. *Nucl. Data Sheets* 120, 211–214.
- Bruccoli, M., Danzeca, S., Brugger, M., Masi, A., Pineda, A., Cesari, J., Dusseau, L., Wrobel, F., 2017. Floating gate dosimeter suitability for Accelerator-like environments. *IEEE Trans. Nucl. Sci.* <https://doi.org/10.1109/TNS.2017.2681651>.
- Cangialosi, C., Danzeca, S., Bruccoli, M., Brugger, M., Masi, A., 2018. Thermal neutron SRAM detector characterization at the CERN Mixed Field Facility, CHARM. *IEEE Trans. Nucl. Sci.* <https://doi.org/10.1109/TNS.2018.2829631>.
- CERN, 2017a. IRRAD website. <https://ps-irrad.web.cern.ch/> (accessed 17 July 2017).
- CERN, 2017b. CHARM website. <http://charm.web.cern.ch/> (accessed 17 July 2017).
- Ferrari, A., Sala, P.R., Fassò, A., Ranft, J., 2005. FLUKA: a multi-particle transport code, CERN 2005-10 (2005), INFN/TC.05/11, SLAC-R-773.
- Gkotsis, B., Glaser, M., Lima, P., Matli, E., Moll, M., Ravotti, F., 2014. A New High-intensity Proton Irradiation Facility at the CERN PS East Area. *Proc. of Scie.* Available online: [https://pos.sissa.it/archive/conferences/213/354/TIPP2014\\_354.pdf](https://pos.sissa.it/archive/conferences/213/354/TIPP2014_354.pdf). (accessed 17 July 2017).
- Holmes-Siedle, A., Adams, L., Pauly, B., Marsden, S., 1985. Linearity of p-MOS radiation dosimeters operated at zero bias. *Electron. Lett.* 21 (13), 570–571.
- Infantino, A., García Alía, R., Brugger, M., 2017a. Monte carlo evaluation of single event effects in a deep-submicron bulk technology: comparison between atmospheric and accelerator environment. *IEEE Trans. Nucl. Sci.* 64 (1), 596–604.
- Infantino A., 2017b. FLUKA Monte Carlo Modelling of the CHARM Facility's Test Area: Update of the Radiation Field Assessment. CERN-ACC-NOTE-2017-0059.
- Jaksic, A., Kimoto, Y., Mohammadzadeh, A., Hajdas, W., 2006. RadFET responses to proton irradiation under different biasing conditions. *IEEE Trans. Nucl. Sci.* 53 (4), 2004–2007.
- Kramer, D., Brugger, M., Klupak, V., Pignard, C., Roede, K., Spiezia, G., Viererbl, L., Wijnands, T., 2011. LHC RadMon SRAM detectors used at different voltages to determine the thermal neutron to high energy hadron fluence ratio. *IEEE Trans. Nucl. Sci.* 58, 1117–1122.
- Marzo, M., Bonaldo, S., Brugger, M., Danzeca, S., Garcia Alia, R., Infantino, A., Thornton, A., 2018. RadFET dose response in the CHARM mixed-field: FLUKA MC simulations. *EPJ Nucl. Sci. Technol.* <https://doi.org/10.1051/epjn/2017016>. (In Press).
- Mekki, J., Dusseau, L., Glaser, M., Guatelli, S., Moll, M., Pia, M.G., Ravotti, F., 2009. Packaging effects on RadFET sensors for high energy physics experiments. *IEEE Trans. Nucl. Sci.* 56 (4), 2061–2069.
- Mekki, J., Brugger, M., Danzeca, S., Dusseau, L., Roede, K., Spiezia, G., 2013. Mixed

- particle field influence on RadFET responses using Co-60 calibration. *IEEE Trans. Nucl. Sci.* 60 (4), 2435–2443.
- Mekki, J., Brugger, M., Alia, R.G., Thornton, A., Dos Santos Mota, N.C., Danzeca, S., 2016. CHARM: a mixed field facility at CERN for radiation tests in ground, atmospheric, space and accelerator representative environments. *IEEE Trans. Nucl. Sci.* 63 (4), 2106–2114.
- Ravotti, F., 2018. Dosimetry techniques and radiation test facilities for total ionizing dose testing. *IEEE Trans. Nucl. Sci.* <https://doi.org/10.1109/TNS.2018.2829864>.
- Spiezia, G., Peronnard, P., Masi, A., Brugger, M., Bruccoli, M., Danzeca, A., Garcia Alia, R., Losito, R., Mekki, J., Oser, P., Gaillard, R., Dusseau, L., 2014. A new RadMon version for the LHC and its injection lines. *IEEE Trans. Nucl. Sci.* 61 (6), 3424–3431.
- Thornton, A., 2016. CHARM Facility Test Area Radiation Field Description. CERN-ACC-NOTE-2016-12345.
- Vincke, H., Brunner, L., Floret, I., Forkel-Wirth, D., Fuerstner, M., Mayer, S., Theis, C., 2007. Response of alanine and radio-photo-luminescence dosimeters to mixed high-energy radiation fields. *Rad. Prot. Dos.* 125 (1–4), 340–344.
- Yamamoto, T., 2011. RPL Dosimetry: Principles and Applications. In Proc: AIP Conference Proceedings 1345, 217, <<http://dx.doi.org/10.1063/1.3576169>>.